

Supporting information for

**Effect of solvent, temperature and pressure on stability of chiral and
perovskite metal formate frameworks of $[\text{NH}_2\text{NH}_3][\text{M}(\text{HCOO})_3]$
($\text{M}=\text{Mn, Fe, Zn}$)**

*Mirosław Maczka,^{*a} Katarzyna Pasińska,^a Maciej Ptak,^a Waldeci Paraguassu,^b Tercio Almeida
da Silva,^b Adam Sieradzki,^c and Adam Pikul^a*

^a*Institute of Low Temperature and Structure Research, Polish Academy of Sciences, Box 1410,
50-950 Wrocław 2, Poland*

^b*Faculdade de Física, Universidade Federal do Pará, 66075-110, Belém, PA, Brazil*

^c*Department of Experimental Physics, Wrocław University of Technology, Wybrzeże
Wyspiańskiego 27, 50-370, Wrocław, Poland*

e-mail: m.maczka@int.pan.wroc.pl

Table S1. Detailed crystallographic data for perovskite HyFe at 290 K and 360 K.

Chemical formula C ₃ H ₈ FeN ₂ O ₆		
M _r	223.96	223.96
Crystal system	Orthorhombic	Orthorhombic
Space group	Pna2 ₁	Pnma
Temperature (K)	290	360
a, b, c (Å)	8.811 (3), 7.782 (2), 8.735 (4), 11.763 (5), 11.657 (3)	7.871 (3)
V(Å ³)	799.34 (4)	808.84 (6)
Z	4	4
Radiation type	Mo Kα	Mo Kα
m (mm ⁻¹)	1.88	1.86
Crystal size (mm)	0.35 × 0.33 × 0.29	0.20 × 0.17 × 0.15
Diffractometer	Xcalibur, Atlas	Xcalibur, Atlas
Absorption correction	Analytical	Analytical
T _{min} , T _{max}	0.563, 0.639	0.769, 0.813
No. of measured, independent and observed	7617, 1573, 1409	4860, 842, 655
[I > 2s(I)] reflections		
R _{int}	0.025	0.023
(sin q/l) _{max} (Å ⁻¹)	0.617	0.617
R[F ² > 2s(F ²)], wR(F ²), S	0.020, 0.051, 1.06	0.028, 0.079, 1.11
No. of reflections	1573	842
No. of parameters	111	74
No. of restraints	1	4
Dρ _{max} , Dρ _{min} (e Å ⁻³)	0.19, -0.21	0.17, -0.30
Absolute structure parameter	0.054 (11)	

Table S2 Detailed crystallographic data for chiral HyFe at 360 K.

Chemical formula C₃H₈FeN₂O₆	
M _r	223.96
Crystal system	Hexagonal
Space group	P6 ₃
Temperature (K)	360
a, b, c (Å)	7.946 (3), 7.946 (3), 7.618 (3)
V (Å ³)	416.6 (4)
Z	2
Radiation type	Mo Kα
m (mm ⁻¹)	1.81
Crystal size (mm)	0.35 × 0.21 × 0.17
Diffractometer	Xcalibur, Atlas
Absorption correction	Analytical
T _{min} , T _{max}	0.646, 0.796
No. of measured, independent and observed [I > 2s(I)] reflections	3723, 711, 617
R _{int}	0.031
(sin q/l) _{max} (Å ⁻¹)	0.691
R[F ² > 2s(F ²)], wR(F ²), S	0.029, 0.062, 1.05
No. of reflections	711
No. of parameters	50
No. of restraints	8
Δρ _{max} , Δρ _{min} (e Å ⁻³)	0.22, -0.27
Absolute structure parameter	-0.030 (19)

Table S3 Detailed crystallographic data for chiral HyMn at 100 K and 310 K.

<i>Chemical formula</i>	C ₁₂ H ₃₂ Mn ₄ N ₈ O ₂₄	C ₃ H ₈ MnN ₂ O ₆
-------------------------	--	---

M_r	892.21	223.05
Crystal system	Monoclinic	Hexagonal
Space group	$P2_1$	$P6_3$
Temperature (K)	100	310
a, b, c (Å)	16.137 (5), 16.140 (5)	7.605 (3), 7.988 (3), 7.988 (3), 7.807 (3)
β (°)	119.98 (3)	
V (Å ³)	1715.7 (10)	431.4 (4)
Z	2	2
Radiation type	Mo $K\alpha$	Mo $K\alpha$
μ (mm ⁻¹)	1.54	1.52
Crystal size (mm)	0.19 × 0.14 × 0.14	0.19 × 0.14 × 0.14
Diffractometer	Xcalibur, Atlas	Xcalibur, Atlas
Absorption correction	Multi-scan	Analytical
T_{\min}, T_{\max}	0.874, 1.000	0.821, 0.870
No. of measured, independent and observed [$I > 2s(I)$] reflections	24249, 6731, 6380	8258, 567, 544
R_{int}	0.038	0.028
(sin q/l) _{max} (Å ⁻¹)	0.617	0.616
$R[F^2 > 2s(F^2)], wR(F^2), S$	0.029, 0.058, 1.04	0.017, 0.042, 1.10
No. of reflections	6731	567
No. of parameters	477	50
No. of restraints	40	2
$\Delta\rho_{\max}, \Delta\rho_{\min}$ (e Å ⁻³)	0.30, -0.38	0.17, -0.18
Absolute structure parameter	-0.017 (8)	0.000 (12)

Table S4 The geometries of the N-H···O hydrogen bonds between the NH₂NH₃⁺ cations and the anionic framework in the perovskite HyFe (distances, Å; angles, °) at 290 K (LT phase) and 360 K (HT phase).

D—H···A	D—H	H···A	D···A	D—H···A
LT phase, <i>Pna2</i> ₁				
N1—H1A···O4ⁱ	0.89	2.10	2.933 (6)	154.9
N1—H1B···O1	0.89	2.42	2.970 (6)	119.9
N1—H1B···O2	0.89	2.06	2.940 (5)	169.8
N1—H1C···O5ⁱⁱ	0.89	2.06	2.893 (4)	155.6
N2—H2A···O6ⁱⁱ	0.86	2.46	3.128 (5)	134.4
N2—H2B···O3ⁱ	0.86	2.35	3.049 (5)	138.0
Symmetry codes: (i) $-x-1/2, y+1/2, z-1/2$; (ii) $x+1/2, -y-3/2, z$.				
HT phase, <i>Pnma</i>				
N1—H1A···O1ⁱ	0.877 (19)	2.29 (3)	3.013 (3)	140 (3)
N1—H1A···O1ⁱⁱ	0.877 (19)	2.29 (3)	3.013 (3)	140 (3)
N1—H1B···O3	0.886 (19)	2.09 (2)	2.946 (3)	163 (4)
N1—H1B···O2	0.886 (19)	2.40 (3)	3.112 (3)	137 (3)
N2—H2B···O2ⁱⁱⁱ	0.88 (2)	2.42 (6)	3.083 (6)	133 (6)
Symmetry codes: (i) $x, y, z+1$; (ii) $x, -y+1/2, z+1$; (iii) $x, -y+1/2, z$.				

Table S5. Selected bond distances (Å) and bond angles (°) of LT (290K) and HT (360K) phases of perovskite HyFe.

Parameter	290 K, <i>Pna2</i>₁	360 K, <i>Pnma</i>
------------------	---------------------------------------	---------------------------

Fe–O	2.129 (2)-2.146 (2)	2.1337 (13) Å -2.1527 (14)
C–O	1.236 (4)-1.258 (5)	1.235 (3)-1.246 (3)
N–N	1.428 (5)	1.381 (9)
<i>cis</i> -O–Fe–O	86.91(10)-93.96 (10)	87.83 (6)- 92.17 (6)
<i>trans</i> -O–Fe–O	178.34 (12)-179.21 (11)	180
O–C–O	125.2 (3)-126.2 (3)	125.6 (3)-125.9 (2)
Fe–O–C	118.9 (2)-123.4 (2)	121.48 (15)-122.18(14)
Fe–OCHO–Fe (Fe···Fe)	5.847-5.881	5.879-5.882

Table S6. Selected bond distances (Å) and bond angles (°) of the HT (360K) phase of chiral HyFe.

Parameter	360 K, <i>P6₃</i>
Fe–O	2.122 (3) - 2.123 (3)
C–O	1.228 (6)-1.232 (6)
N–N	1.358 (12)
<i>cis</i> -O–Fe–O	83.02 (9)- 92.52 (10)
<i>trans</i> -O–Fe–O	173.41 (9)
O–C–O	127.5 (4)
Fe–O–C	125.9 (3) - 126.0 (3)
Fe–OCHO–Fe (Fe···Fe)	5.963

Table S7. Selected bond distances (Å) and bond angles (°) of LT (100K) and HT (310K) phases of HyMn.

Parameter	100 K, <i>P2₁</i>	310 K, <i>P6₃</i>
Mn–O	2.139 (5) - 2.195 (5)	2.174 (13) Å
C–O	1.232 (10) - 1.269 (9)	1.230 (4) - 1.235 (4)

N–N	1.447 (6) - 1.454 (4)	1.338 (18)
<i>cis</i> -O–Mn–O	79.17(16) - 95.85 (19)	82.51 (7) - 93.18 (8)
<i>trans</i> -O–Mn–O	169.04 (19) - 173.30 (16)	172.60 (7)
O–C–O	123.6 (7) - 126.5 (7)	127.5 (3)
Mn–O–C	119.0 (4) - 131.2 (5)	125.4 (2) - 125.6 (2)
Mn–OCHO–Mn (Mn···Mn)	5.921 - 6.108	6.042

Table S8. The geometries of the N-H···O and N-H···N hydrogen bonds between the NH₂NH₃⁺ cations and the anionic framework in the chiral HyFe (distances, Å; angles, °) at 360 K (HT phase).

D—H···A	D—H	H···A	D···A	D—H···A
HT phase, P6 ₃				
N1—H1A···O1	0.86	2.17	2.91 (6)	143.6
N1—H1B···O1ⁱ	0.86	2.34	2.98 (5)	131.3
N1—H1B···O2ⁱⁱ	0.86	2.42	3.16 (5)	144.3
N2—H2A···O1ⁱⁱⁱ	0.89	2.36	3.13 (3)	145.9
N2—H2B···O2^{iv}	0.89	2.17	2.92 (4)	141.7
N2—H2C···O2^v	0.89	2.38	3.02 (3)	128.7
N2—H2B···N1^{iv}	0.89	2.40	2.96 (3)	121.0

Symmetry codes: (i) -x+y, -x, z; (ii) y, -x+y, z+1/2; (iii) -y, x-y, z; (iv) x-y, x, z+1/2; (v) -x, -y, z+1/2.

Table S9. The geometries of the N-H···O hydrogen bonds between the NH₂NH₃⁺ cations and the anionic framework in HyMn (distances, Å; angles, °) of the LT (100K) and HT (310K) phases of HyMn.

D—H···A	D—H	H···A	D···A	D—H···A
LT phase, P2 ₁				

N1—H1B···O4	0.87	2.00	2.813 (7)	154.0
N1—H1A···O16^{iv}	0.87	2.01	2.865 (7)	166.0
N2—H2B···N1ⁱ	0.91	2.25	3.132 (8)	164.6
N3—H3B···O21ⁱ	0.91	1.97	2.870 (7)	170.0
N3—H3A···O24ⁱⁱⁱ	0.91	1.95	2.798 (7)	155.2
N3—H3C···N4^v	0.91	2.22	3.118 (7)	170.4
N5—H5B···O10	0.91	1.97	2.871 (7)	169.9
N5—H5A···O14^{vi}	0.91	1.94	2.798 (7)	155.8
N5—H5C···N6^{vii}	0.91	2.21	3.110 (7)	169.3
N7—H7B···O7	0.91	2.18	2.807 (16)	125.0
N7—H7C···O20^{vi}	0.91	2.33	2.905 (16)	121.3
N7—H7A···N8^{vi}	0.91	2.11	2.73 (2)	125.1
N8—H8A···O1^{vi}	0.88	2.16	3.01 (2)	165.7
N8—H8B···N7ⁱⁱ	0.87	2.06	2.73 (2)	133.9
N9—H9A···O1^{vi}	0.91	2.16	2.809 (17)	127.4
N9—H9B···O19	0.91	2.33	2.927 (18)	123.1
N9—H9C···N10^{vi}	0.91	2.10	2.76 (2)	127.8
N10—H10A···O13^{vi}	0.87	2.14	3.00 (2)	172.9
N10—H10B···N9ⁱⁱ	0.88	2.03	2.76 (2)	139.7
N11—H11A···O1^{vi}	0.86	2.29	2.95 (2)	133.7
N11—H11B···O7	0.86	2.14	3.00 (2)	172.7
N12—H12A···O6^{vi}	0.91	2.19	2.919 (16)	136.6
N12—H12C···O13^{vi}	0.91	2.02	2.801 (16)	142.9
N12—H12B···N11^{vi}	0.91	2.04	2.78 (2)	136.8

Symmetry codes: (i) $-x+2, y-1/2, -z+1$; (ii) $-x+2, y+1/2, -z$; (iii) $x-1, y-1, z$; (iv) $-x+2, y+1/2, -z+1$; (v) $-x+1, y+1/2, -z+1$; (vi) $-x+2, y-1/2, -z$; (vii) $-x+1, y+1/2, -z$.

HT phase, $P6_3$

N1—H1A···O1	0.86	2.11	2.91 (6)	154.1
N1—H1B···O1ⁱ	0.86	2.35	3.00 (6)	132.9
N1—H1B···O2ⁱⁱ	0.86	2.47	3.24 (4)	150.3
N2—H2A···O1ⁱⁱⁱ	0.89	2.36	3.18 (3)	152.7
N2—H2B···O2^{iv}	0.89	2.07	2.88 (5)	150.8
N2—H2C···N1ⁱⁱ	0.89	2.46	3.049 (17)	124.3

Symmetry codes: (i) $-x+y, -x, z$; (ii) $y, -x+y, z+1/2$; (iii) $-y, x-y, z$; (iv) $x-y, x, z+1/2$.

Table S10. IR frequencies (in cm^{-1}) of the studied compounds at room-temperature and suggested assignments.^a

HyMn perovskite	HyFe perovskite	HyZn perovskite	HyMn chiral	HyFe chiral	HyZn chiral	assignment
3330w	3330w	3331w	3347w	3342w	3339w	$\nu(\text{NH}_2)$ and $\nu(\text{NH}_3)$
3280vw	3280vw	3271w	3283w	3281w	3274w	$\nu(\text{NH}_2)$ and $\nu(\text{NH}_3)$

3206vw	3203vw	3198vw	3163w,b	3164sh		v(NH ₂) and v(NH ₃)
3091w	3093w	3092w	3090w,b	3078m,b	3071m,b	v(NH ₂) and v(NH ₃)
3010m,b	3009m,b	3011m,b				v(NH ₂) and v(NH ₃)
2980sh	2974sh	2975sh	2974m,b	2961m,b	2971m,b	v(NH ₂) and v(NH ₃)
2940w	2940w	2940w				v(NH ₂) and v(NH ₃)
2874m	2884m	2887w	2847m	2859m	2880w	v ₁ (HCOO ⁻)
					2841w	
2842w	2835sh	2837w				overtones
2754w	2743w	2748w	2730w	2724w	2728w	overtones
2713vww	2709vww	2712vww				overtones
2635w	2631w	2630w	2625w	2623w	2613w	overtones
1641w	1640m	1641m	1634sh	1632sh	1632w	δ(NH ₂)
1608sh	1607sh	1606sh			1600w	δ _{as} (NH ₃)
1588s	1584vs	1588vs	1582vs	1581vs	1581vs	v ₄ (HCOO ⁻)
1523w	1522w	1523w	1518w	1521w	1514w	δ _s (NH ₃)
1387s	1380s	1380s	1373s	1372s	1388sh,	v ₅ (HCOO ⁻)
1380sh		1375sh			1375sh	
1357s	1358s	1357s	1364s	1363s	1365s	v ₂ (HCOO ⁻)
					1359s	
1247vww	1241vww	1245w				τ(NH ₂)
1125sh	1122sh	1122m	1111m	1109m	1114sh	ρ(NH ₂) + ρ(NH ₃)
1111m	1109m	1109m			1104m	ρ(NH ₂) + ρ(NH ₃)
1084sh			1087sh	1085sh	1083sh	ρ(NH ₃)
1066w	1065w	1067w			1071w	v ₆ (HCOO ⁻)
941m	939m	941m	963m	961m	961m	v(NN)
805sh		814sh			812s	v ₃ (HCOO ⁻)

797s	805s	807s	798s	807s	805s	$\nu_3(\text{HCOO}^-)$
					798sh	$\nu_3(\text{HCOO}^-)$

^aKey: s, strong; m, medium; w, weak; vw, very weak; sh, shoulder; b, broad. ν_1 , ν_2 , ν_3 , ν_4 , ν_5 and ν_1 internal modes of the HCOO^- ion correspond to the C-H stretching, symmetric C-O stretching, symmetric O-C-O bending (scissor), antisymmetric C-O stretching, C-H in-plane bending and the C-H out-of-plane bending mode, respectively. ν_s , ν_{as} , δ , ρ , ω and τ denote symmetric stretching, antisymmetric stretching, scissoring, rocking, wagging and twisting vibrations.

Table S11. Raman frequencies (in cm^{-1}) of the studied compounds at room-temperature and suggested assignments.

HyMn perovskite	HyFe perovskite	HyZn perovskite	HyMn chiral	HyFe chiral	HyZn chiral	assignment
3327vw	3329w	3329w	3340vw	3331sh	3335w	$\nu(\text{NH}_2)$ and $\nu(\text{NH}_3)$
3283vw	3281w	3281w	3286vw	3280w	3276w	$\nu(\text{NH}_2)$ and $\nu(\text{NH}_3)$
3236vw	3245w	3241vw				$\nu(\text{NH}_2)$ and $\nu(\text{NH}_3)$

3042vw		3042vw		3050w	3045w	$\nu(\text{NH}_2)$ and $\nu(\text{NH}_3)$
2965w	2967w	2965w	2956w	2954w	2966w	$\nu(\text{NH}_2)$ and $\nu(\text{NH}_3)$
2876m	2886m	2889m	2852m	2867m	2881m	$\nu_1(\text{HCOO}^-)$
					2841m	
2754w		2758w			2754w	overtones
	2737w	2735w	2725w	2722w	2732w	overtones
1644w	1638w	1643w	1631w	1636w	1639w	$\delta(\text{NH}_2)$
1609vw	1608w	1608w		1613w	1622w	$\delta_{\text{as}}(\text{NH}_3)$
1555w	1560w	1548w	1567w	1565w	1565w	$\delta_{\text{as}}(\text{NH}_3)$
1522w	1523vw	1520w	1521vw	1519vw	1517w	$\delta_s(\text{NH}_3)$
1428w	1423vw	1428w				overtones
1384sh	1378s	1378m	1373sh	1372s	1380s	$\nu_5(\text{HCOO}^-)$
1380m						
1358s	1359s	1362s	1365s	1366sh	1365m	$\nu_2(\text{HCOO}^-)$
1124w	1120sh	1120sh		1106w	1106m,b	$\rho(\text{NH}_2) + \rho(\text{NH}_3)$
1110w	1108w	1109w	1102m,b	1092w,b	1094m,b	$\rho(\text{NH}_2) + \rho(\text{NH}_3)$
1067w	1067w	1067w	1067m	1066w	1072m	$\nu_6(\text{HCOO}^-)$
					1065w	
941m	940m	940m	964m	959m	962m	$\nu(\text{NN})$
800m	806m	808m	796m	805m	811sh	$\nu_3(\text{HCOO}^-)$
794m	801m	802m			805m	$\nu_3(\text{HCOO}^-)$
					801sh	$\nu_3(\text{HCOO}^-)$
239w		261w				$T'(\text{HCOO}^-)$
		219sh		223w	204sh	$T'(\text{HCOO}^-)$
184m		207m				$L(\text{HCOO}^-)$
172sh				156sh	179w	$L(\text{HCOO}^-)$
159s	176s	174s	150s	132s	133s	$L(\text{HCOO}^-)$

122m	131w		127s		126sh	L(HCOO ⁻)
110m	110m	125m		91m		L(HCOO ⁻)
	93w					L(HCOO ⁻)
	72m					L(HCOO ⁻)

Table S12. Raman frequencies (in cm⁻¹) of perovskite HyFe, chiral HyMn and chiral HyZn at 80 and 380 K together with suggested assignments.^a

HyFe perovskite		HyFe chiral		HyMn chiral		assignment
380 K	80 K	380 K	80 K	380 K	80 K	
3336vw	3326w	3326sh	3344w	3328vw	3344w	v(NH ₂) and v(NH ₃)
3291w	3281w	3274w	3284w	3277vw	3286w	v(NH ₂) and v(NH ₃)
3245w	3240w					v(NH ₂) and v(NH ₃)

	3203vw	3188w	3156w	3193w	3174w	$\nu(\text{NH}_2)$ and $\nu(\text{NH}_3)$
	3063vw		3061w		3062w	$\nu(\text{NH}_2)$ and $\nu(\text{NH}_3)$
	3008w					
2961w	2971w	2956w	2956w	2958w	2955w	$\nu(\text{NH}_2)$ and $\nu(\text{NH}_3)$
	2949w					
2908sh	2917w					$\nu(\text{NH}_2)$ and $\nu(\text{NH}_3)$
2883m	2892m	2861m	2880m	2851m	2855m	$\nu_1(\text{HCOO}^-)$
	2884sh		2865m			
			2840w		2841w	$\nu_1(\text{HCOO}^-)$
1641w	1655vw	1625w	1646w	1631w	1650w	$\delta(\text{NH}_2)$
	1647w				1613w	
1608w	1604w					$\delta_{\text{as}}(\text{NH}_3)$
1560w	1574w	1548w	1568w	1570w	1572w	$\delta_{\text{as}}(\text{NH}_3)$
	1562w					
1520vww	1529vww	1509vww	1522vww	1518vww	1527w	$\delta_s(\text{NH}_3)$
1422vww	1436vww					overtones
1373sh	1380m	1380sh	1380s	1374sh	1376sh	$\nu_5(\text{HCOO}^-)$
					1370m	
1361s	1364m	1367s	1365s	1364s	1364s	$\nu_2(\text{HCOO}^-)$
	1359s		1355sh		1354w	
	1259w					$\tau(\text{NH}_2)$
1108sh	1137w					$\rho(\text{NH}_2) + \rho(\text{NH}_3)$
1097w	1117w	1086w,b	1113w	1084m,b	1126w	$\rho(\text{NH}_2) + \rho(\text{NH}_3)$
			1091w		1111m	
					1093m	
1067w	1068w	1067m	1067m	1067m	1071m	$\nu_6(\text{HCOO}^-)$
					1066sh	

931m	945m	957m	972w	955m	982m	v(NN)
			962m		972m	
					965m	
					948m	
					937m	
804m	809m	803m	809m	798m	798m	$\nu_3(\text{HCOO}^-)$
			800sh			
799sh	803m					$\nu_3(\text{HCOO}^-)$
223sh	230w		230w	265w	290w	$T'(\text{HCOO}^-)$
					192w	$T'(\text{HCOO}^-)$
		154sh	158sh			$L(\text{HCOO}^-)$
171s	194sh	128s	137s	149s	150s	$L(\text{HCOO}^-)$
	182s		123sh			
156sh	163m					$L(\text{HCOO}^-)$
	150m					
123m	132w			119s	125s	$L(\text{HCOO}^-)$
	122w					
110m	110w	83m	94m			$L(\text{HCOO}^-)$
	106w					
84m	99m, 93w					$L(\text{HCOO}^-)$
67m	71m					$L(\text{HCOO}^-)$

Table S13. Wavenumber intercepts at zero pressure (ω_0) and pressure coefficients ($\alpha=d\omega/dP$), obtained from fitting of the experimental data by linear functions, for the two phases of perovskite HyZn.

ambient pressure phase		high-pressure phase		assignment
ω_0 (cm ⁻¹)	α (cm ⁻¹ GPa ⁻¹)	ω_0 (cm ⁻¹)	α (cm ⁻¹ GPa ⁻¹)	
1378.1	2.44	1384.0	0.95	$\nu_5(\text{HCOO}^-)$
1361.5	3.82	1371.2	0.02	$\nu_2(\text{HCOO}^-)$
1365.0	1.22			$\nu_2(\text{HCOO}^-)$
1105.9	1.86	1112.1	0.30	$\rho(\text{NH}_2) + \rho(\text{NH}_3)$
1067.3	2.02	1075.6	0.63	$\nu_6(\text{HCOO}^-)$

940.7	3.80	948.7	0.81	v(NN)
802.5	1.84	802.6	-0.11	v ₃ (HCOO ⁻)
		263.4	12.02	T'(HCOO ⁻)
256.2	8.63	264.7	2.71	T'(HCOO ⁻)
206.9	3.01	221.7	2.19	T'(HCOO ⁻)
173.0	5.48	184.8	1.86	L(HCOO ⁻)
166.3	1.63			L(HCOO ⁻)
149.3	1.97	160.9	-0.82	L(HCOO ⁻)
123.7	2.87	124.1	1.15	L(HCOO ⁻)

Table S14. Wavenumber intercepts at zero pressure (ω_0) and pressure coefficients ($\alpha = d\omega/dP$), obtained from fitting of the experimental data by linear functions, for the two phases of chiral HyZn.

ambient pressure phase		high-pressure phase		assignment
ω_0 (cm ⁻¹)	α (cm ⁻¹ GPa ⁻¹)	ω_0 (cm ⁻¹)	α (cm ⁻¹ GPa ⁻¹)	
1378.1	8.26	1387.2	2.67	v ₅ (HCOO ⁻)
1351.0	16.82	1378.2	1.91	v ₂ (HCOO ⁻)
1071.1	3.21			v ₆ (HCOO ⁻)
1064.8	1.06	1066.8	1.43	v ₆ (HCOO ⁻)

959.1	7.51	968.8	5.61	v(NN)
806.0	2.80	797.4	3.90	$\nu_3(\text{HCOO}^-)$
287.9	6.90			$\text{T}(\text{HCOO}^-)$
201.2	2.73			$\text{T}'(\text{HCOO}^-)$
180.4	-0.43	188.4	7.11	L(HCOO^-)
151.5	3.64			L(HCOO^-)
131.4	-2.84			L(HCOO^-)

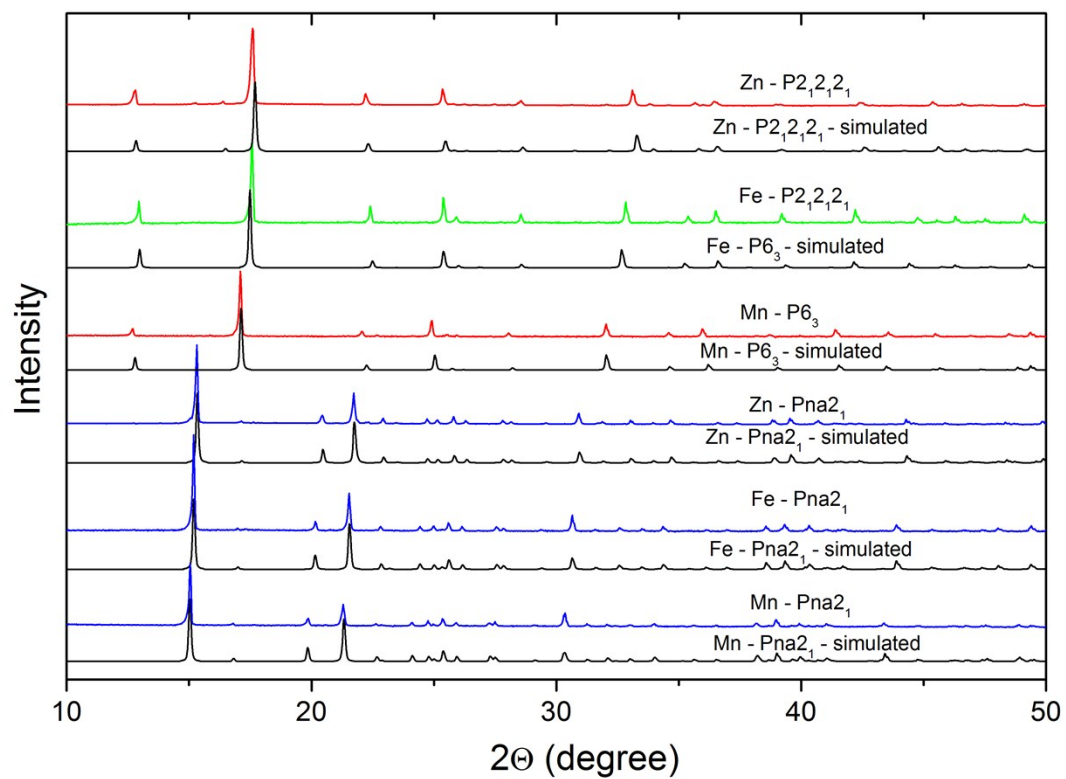


Figure S1. Powder XRD patterns for the as-prepared bulk perovskite- and chiral-type samples of HyZn, HyMn and HyFe together with the calculated ones based on the single crystal structures at room temperature.

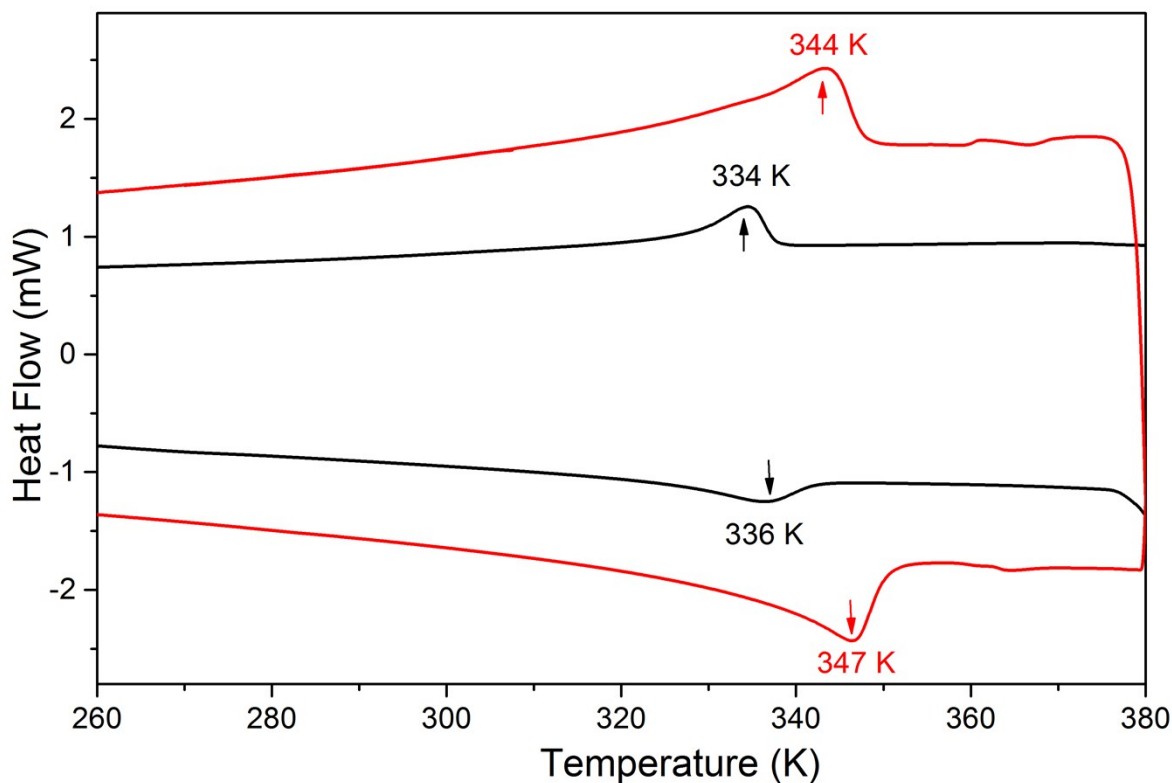


Figure S2. DSC traces for perovskite (red) and chiral (black) HyFe in heating and cooling modes.

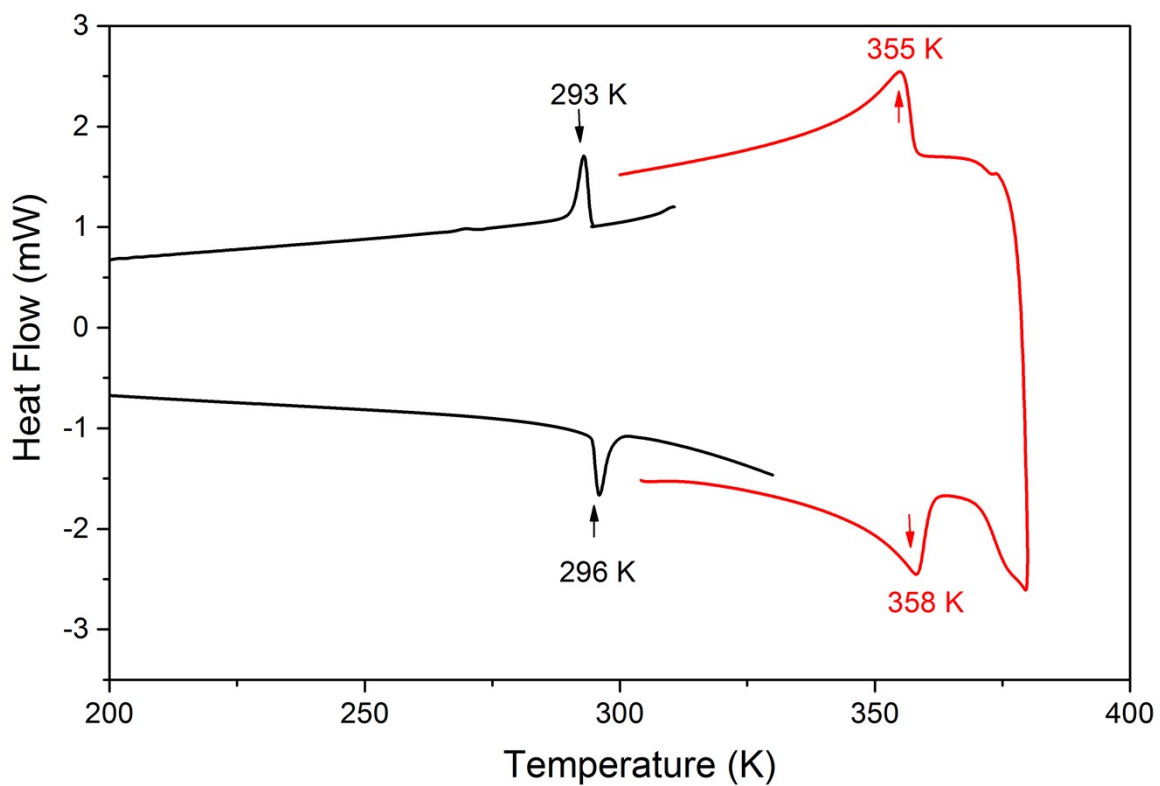


Figure S3. DSC traces for perovskite (red) and chiral (black) HyMn in heating and cooling modes.

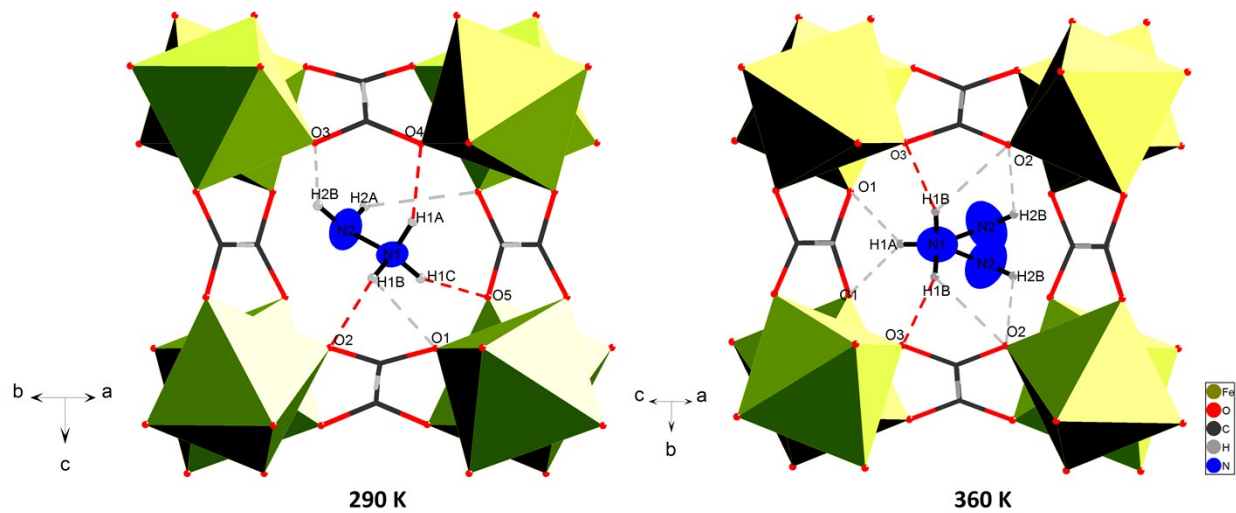


Figure S4. Ordering of the NH_2NH_3^+ counterions with temperature lowering for perovskite HyFe. Site occupation factors are drawn for the nitrogen atoms with 50% probability. Red and grey dashed lines represent strong and weak hydrogen bonds respectively.

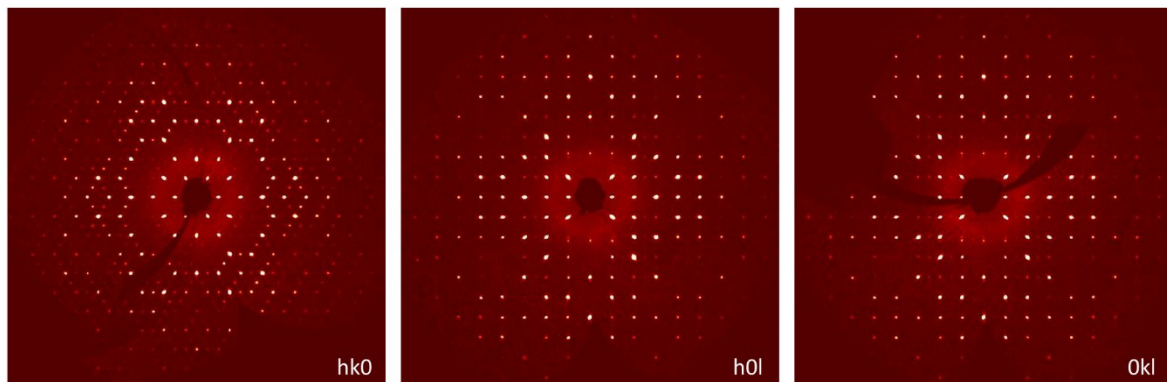


Figure S5. A reconstructed view of the $hk0$, $h0l$ and $0kl$ plane of reciprocal space for the LT of HyFe.

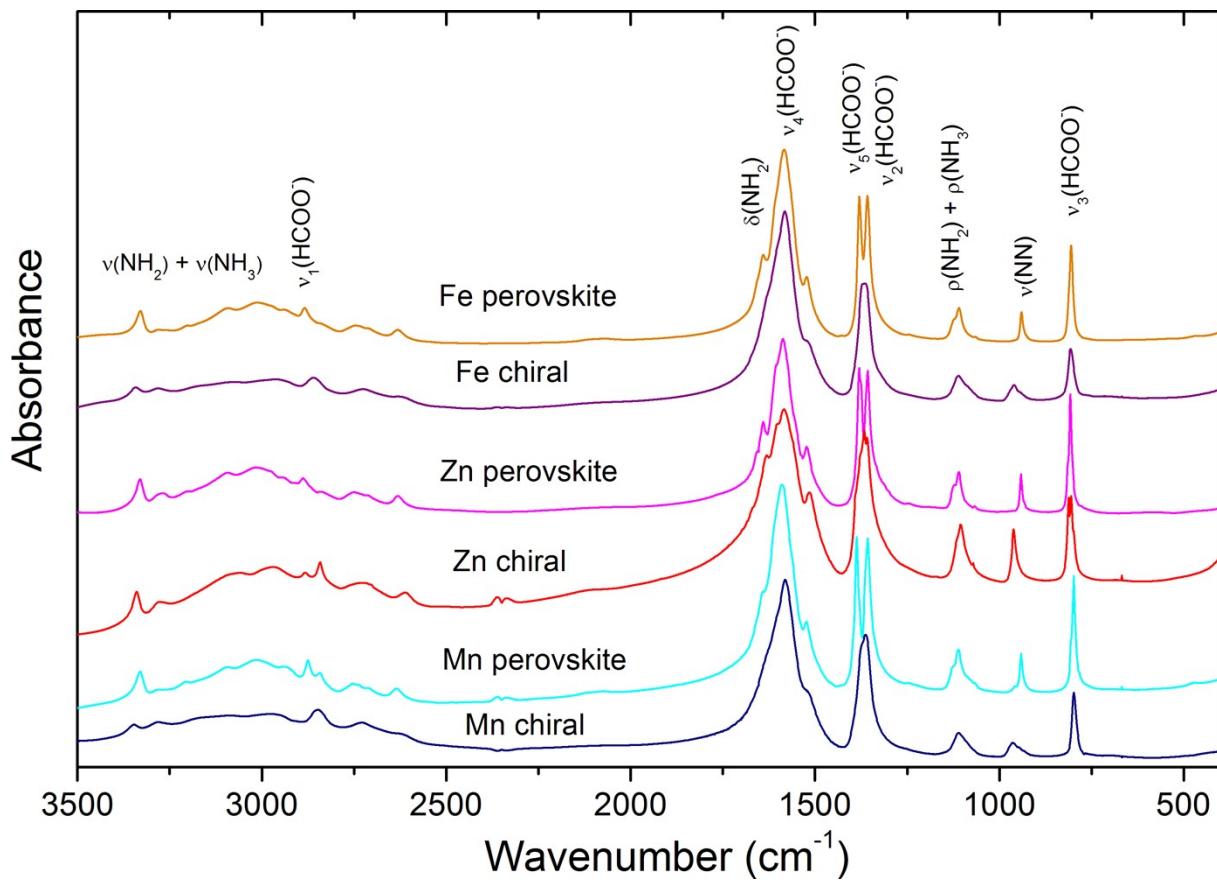


Figure S6. Room-temperature IR spectra in the 3500-400 cm^{-1} range for chiral and perovskite phases of the studied compounds.

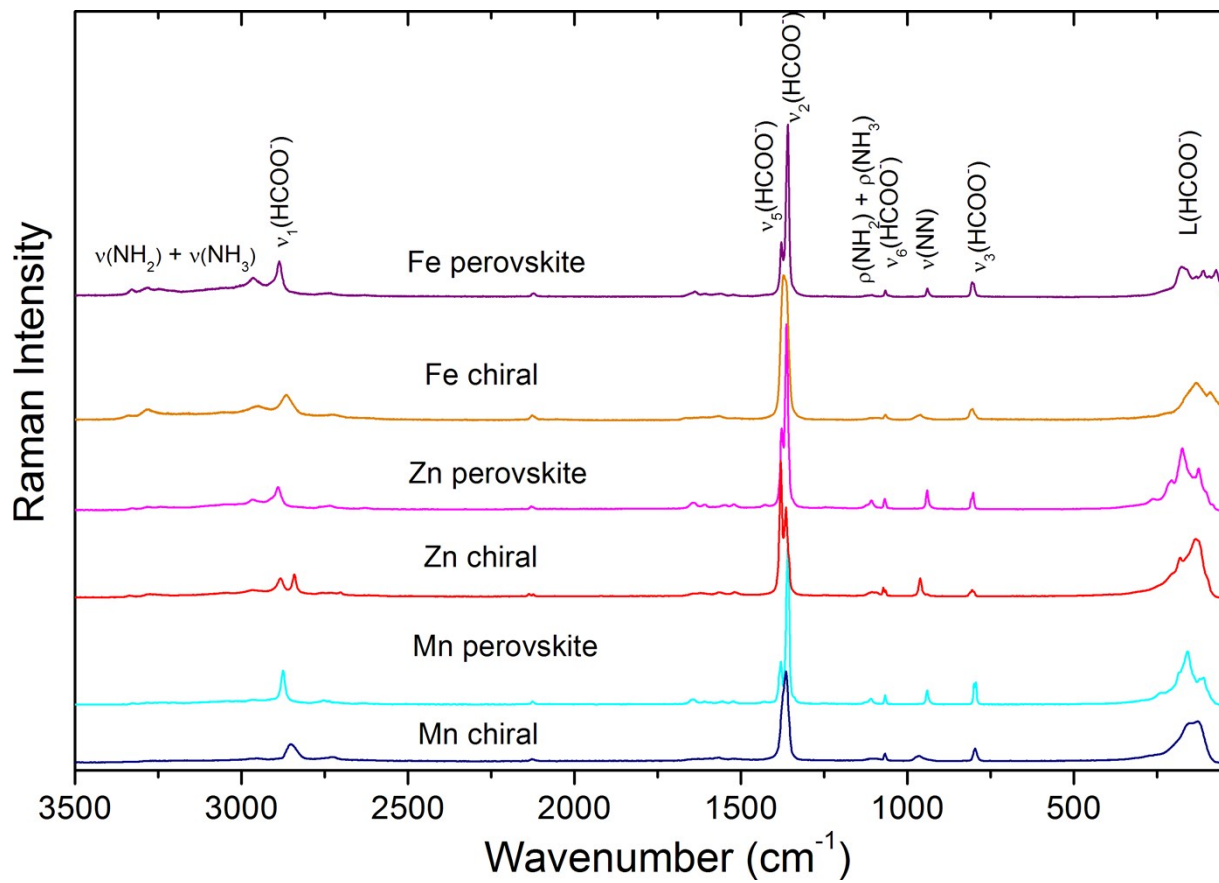


Figure S7. Room-temperature IR spectra in the 3500-50 cm^{-1} range for chiral and perovskite phases of the studied compounds.

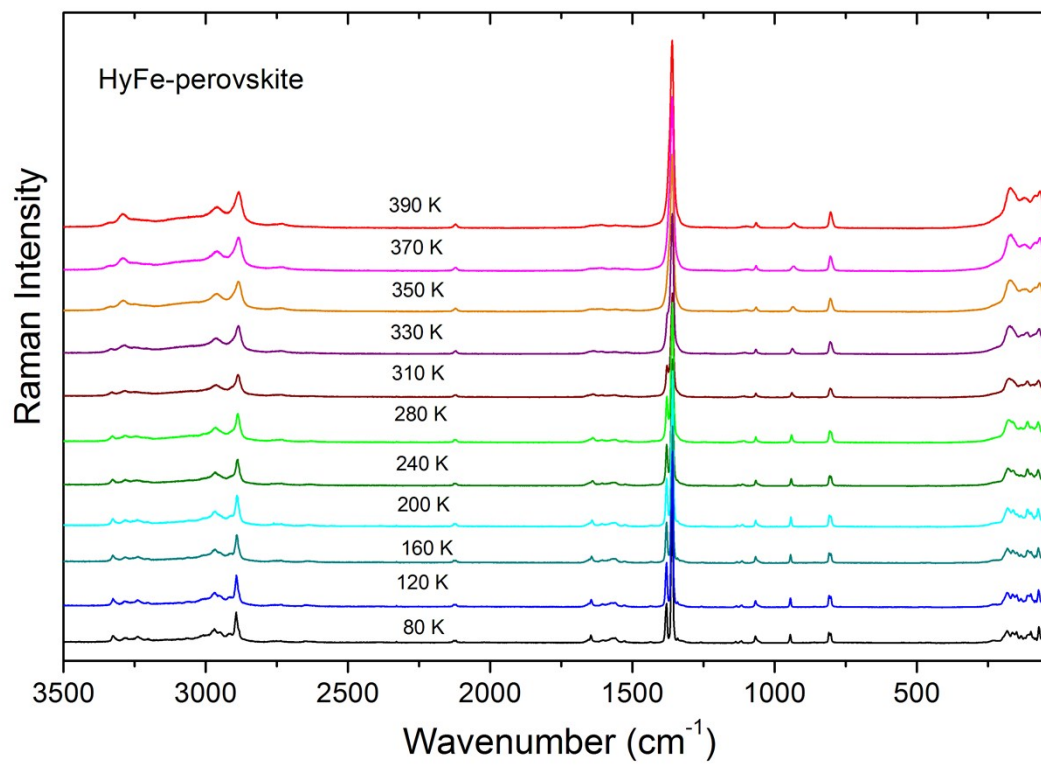


Figure S8. Temperature-dependent Raman spectra of perovskite HyFe in the 3500-50 cm⁻¹ wavenumber range.

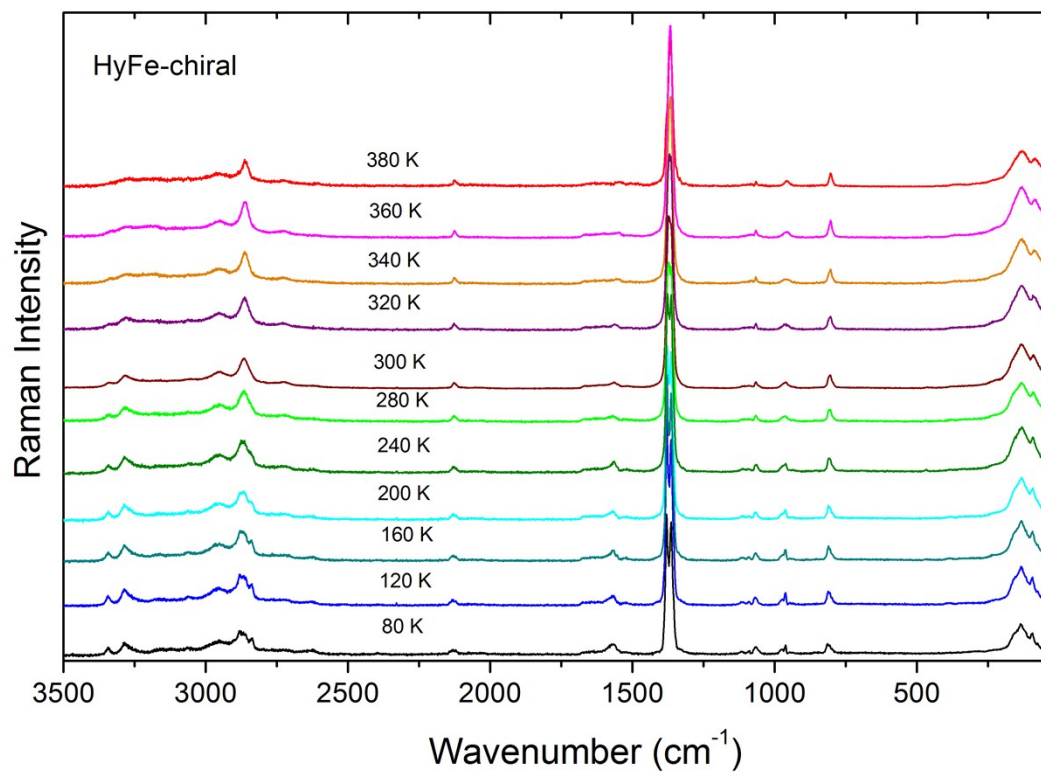


Figure S9. Temperature-dependent Raman spectra of chiral HyFe in the 3500-50 cm⁻¹ wavenumber range.

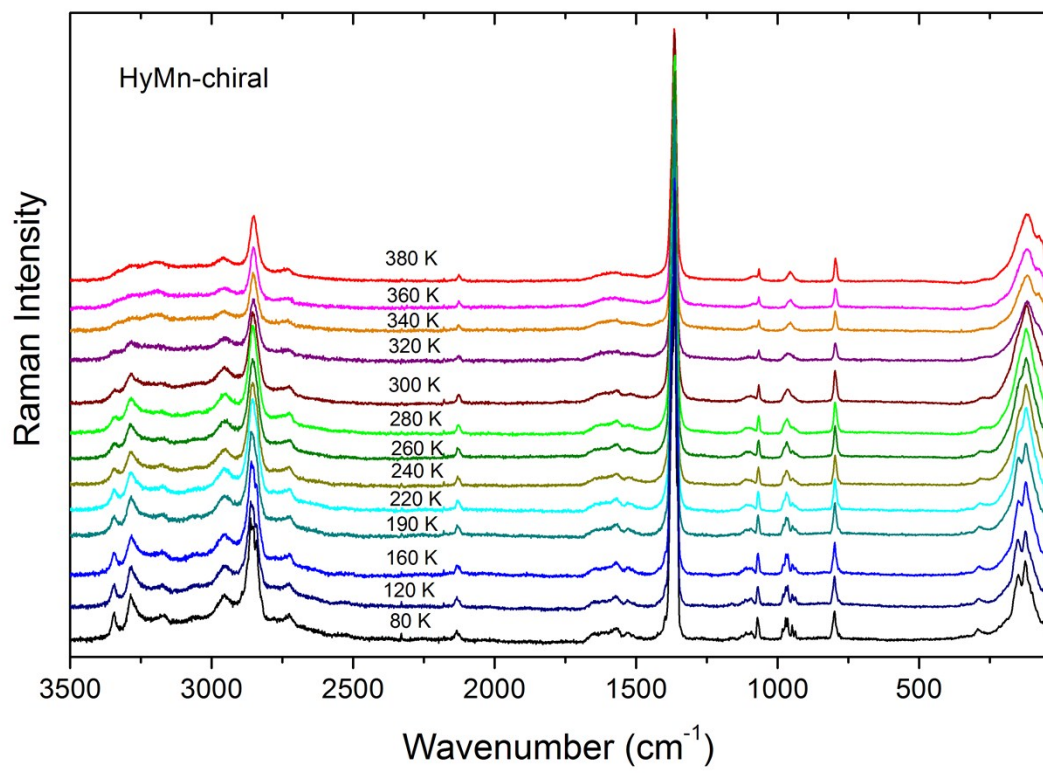


Figure S10. Temperature-dependent Raman spectra of chiral HyMn in the 3500-50 cm⁻¹ wavenumber range.

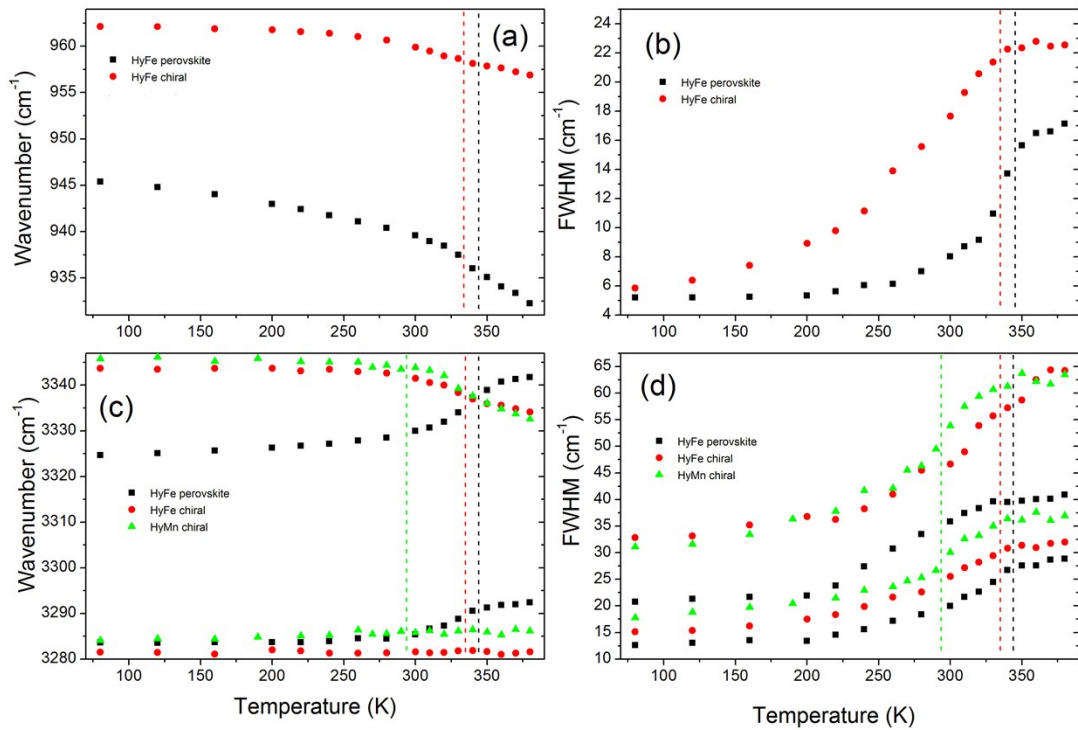


Figure S11. Temperature dependence of Raman wavenumbers (a, c) and FWHM (b, d) for a few selected modes of perovskite HyFe (black squares), chiral HyFe (red circles) and chiral HyMn (green triangles). Vertical dashed lines correspond to the phase transition temperature of perovskite HyFe (black), chiral HyFe (red) and chiral HyMn (green).

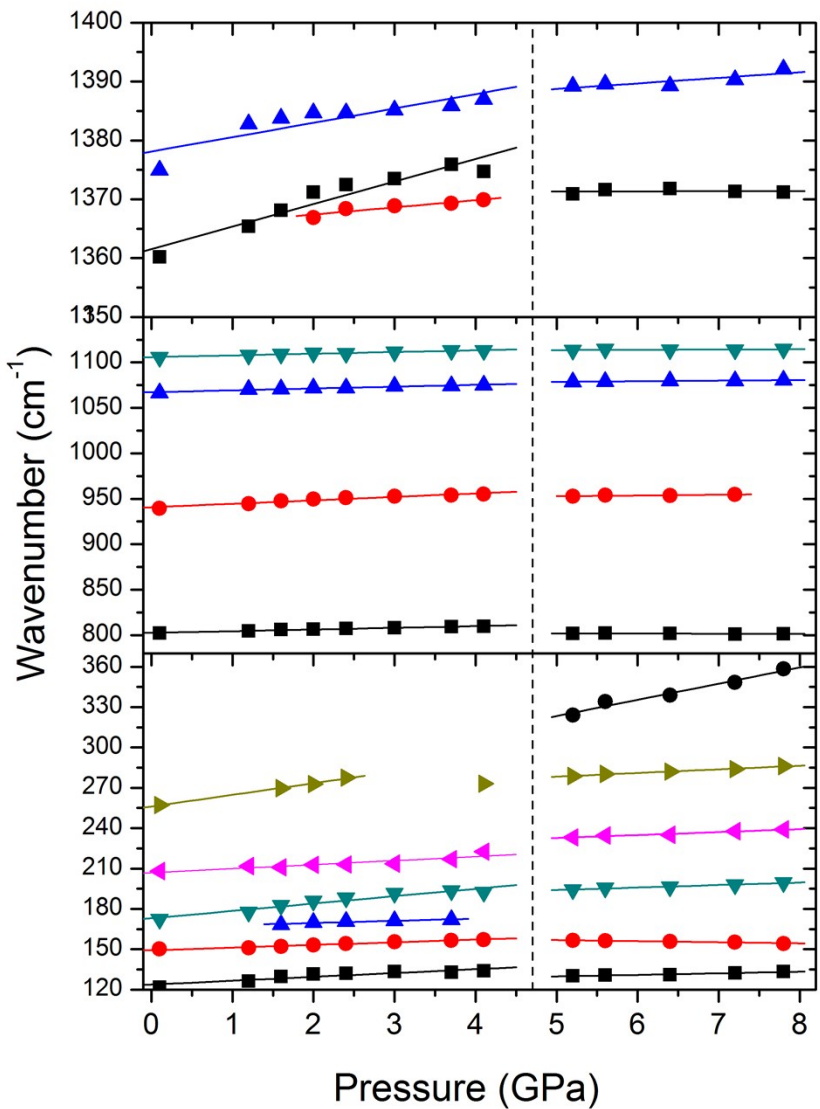


Figure S12. Wavenumber vs. pressure plots of the Raman modes observed in perovskite HyZn crystal for compression experiment. The solid lines are linear fits on the data to $\omega(P) = \omega_0 + \alpha P$. Vertical line shows the pressure at which a structural phase transition occurs.

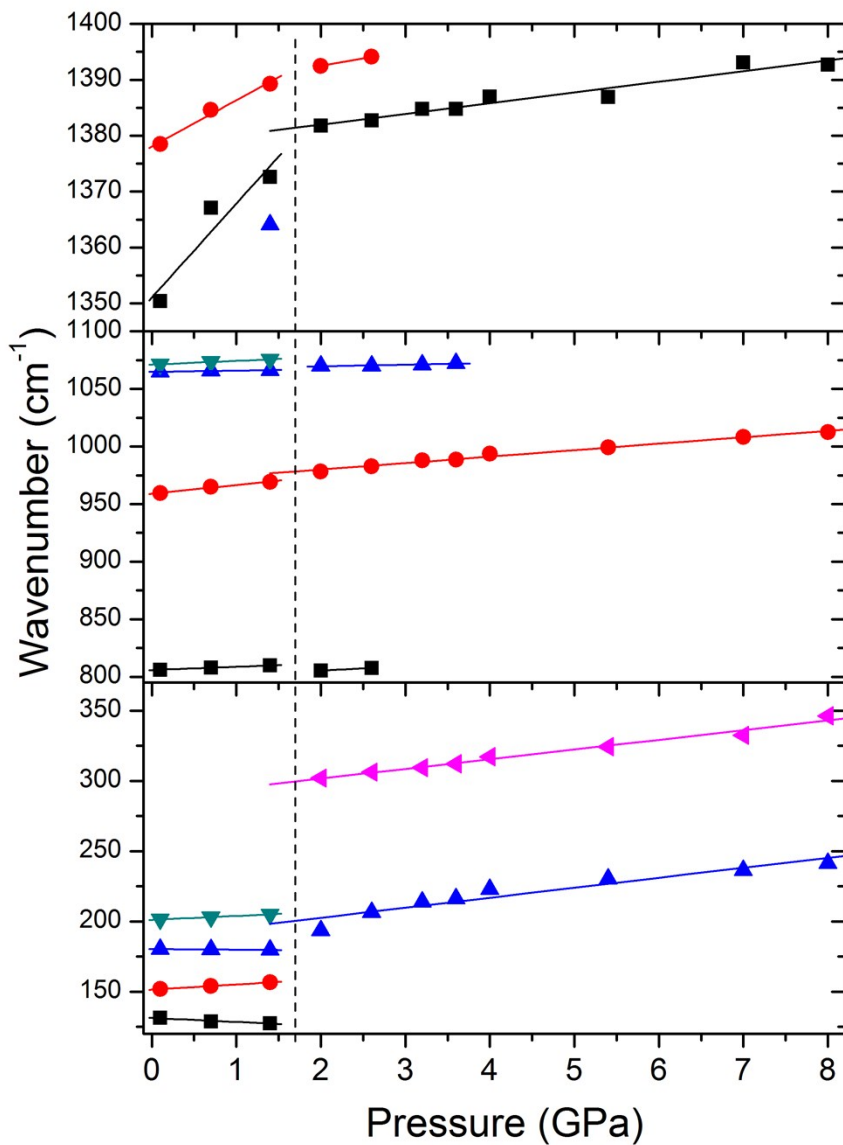


Figure S13. Wavenumber vs. pressure plots of the Raman modes observed in chiral HyZn crystal for compression experiment. The solid lines are linear fits on the data to $\omega(P) = \omega_0 + \alpha P$. Vertical line shows the pressure at which a structural phase transition occurs.

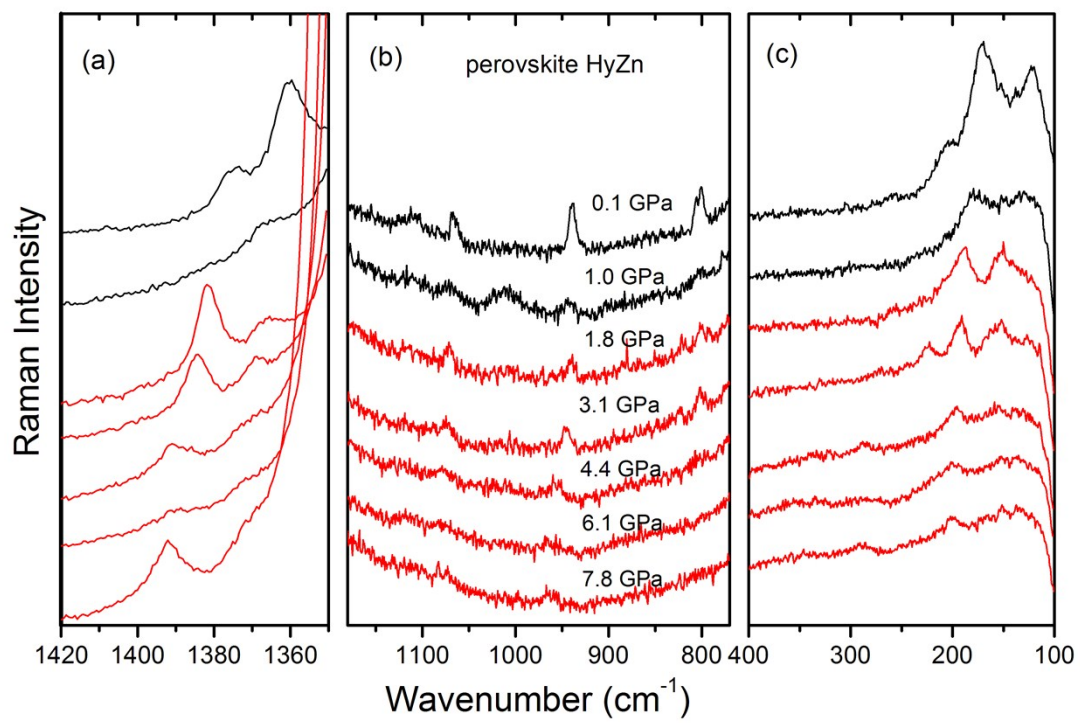


Figure S14. Raman spectra of perovskite HyZn recorded during decompression experiment.

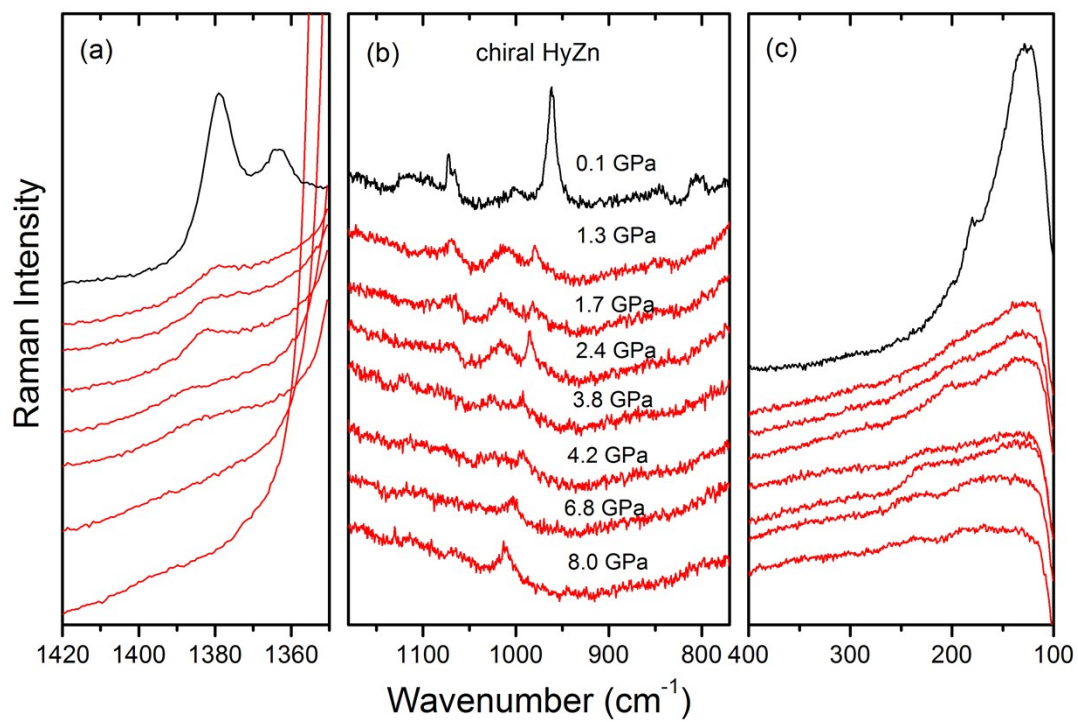


Figure S15. Raman spectra of chiral HyZn recorded during decompression experiment.